A reptation-based model to the dynamics and rheology of linear entangled polymers reinforced with nanoscale rigid particles

Kabanemi, Kalonji K.; Hétu, Jean-François

Publisher's version / Version de l'éditeur:
https://doi.org/10.1016/j.jnnfm.2010.04.006
Journal of Non-Newtonian Fluid Mechanics, 165, 15-16, pp. 866-878, 2010-04-17

J. Non-Newtonian Fluid Mech. 165 (2010) 866–878

Contents lists available at ScienceDirect

Journal of Non-Newtonian Fluid Mechanics

journal homepage: www.elsevier.com/locate/jnnfm

A reptation-based model to the dynamics and rheology of linear entangled polymers reinforced with nanoscale rigid particles

Kalonji K. Kabanemi*, Jean-François Hétu

Industrial Materials Institute (IMI), National Research Council of Canada (NRC) 75 de Mortagne, Boucherville, Québec, Canada J4B 6Y4

ARTICLE INFO

Article history:
Received 31 August 2009
Received in revised form 25 March 2010
Accepted 17 April 2010

Keywords:
Polymer–nanoparticle interactions
Polymer nanocomposites
Rheological modeling
Reptation-based model
Detachment/re-attachment dynamics
Viscoelasticity

ABSTRACT

A reptation-based model, that incorporates transient polymer–nanoparticle surface interactions, is proposed to describe the dynamics and rheological behaviors of linear entangled polymers filled with isotropic rigid nanoscale particles. Dispersed nanoparticles are sufficiently small such that even at low volume fractions, the average particle wall-to-wall distance is on the order of the chain size. The model predicts a scaling law in the form, $\tau_{d,eff} \sim \tau_d(\phi_{ad}N+1)^2$, where $\tau_{d,eff}$ is the effective reptation time of a chain in the presence of attractive nanoparticles, τ_d is its reptation time in the neat polymer, ϕ_{ad} is the fraction of attached monomers per chain, and N is the number of monomers per chain. Hence, the overall relaxation is extremely retarded by attractive nanoparticles in the limit of strongly adsorbed chains. Also, it is found that the effective reptation time, $\tau_{d,eff}$, can be controlled through five main parameters, i.e., the molecular weight of the polymer chain, N, the size of the nanoparticles, d_f, the density of attractive site on the nanoparticle surface, n_{as}, the monomer–nanoparticle energetic interaction, ε, and the nanoparticle volume fraction, ϕ_f. The nonequilibrium dynamics of detachment/re-attachment of monomers from/to nanoparticle surfaces under flow conditions is incorporated in the model to elucidate the effect of monomer–surface interactions on the nonlinear viscoelastic behavior. The resulting model correctly captures the linear dynamical properties and shear rheological behaviors of nanocomposite systems studied. Under very slow shear flow conditions, these filled systems exhibit a strong non-Newtonian behavior and a large enhancement in the viscosity as a certain number of monomers in the chain are attached to nanoparticle surfaces, while at very high shear rates, the neat polymer dominates the shear thinning behavior, suggesting that addition of nanoparticles contributes negligible to the viscosity in strong flows. A picture that is based on transient polymer–particle surface interactions, i.e., the detachment/re-attachment dynamics of monomers from/to nanoparticle surfaces is proposed to interpret the observed huge alteration in rheological properties.

1. Introduction

During the recent past, polymers filled with nanoparticles have attracted considerable technological and scientific interest because of dramatic enhancements in physical, thermal, and mechanical properties observed experimentally. To investigate the microscopic reasons underlying these macroscopic properties and to improve the manufacturing procedure of such mixtures, it is of interest to understand in detail the dynamics and conformational changes of entangled polymer chains close to a solid surface along with, the influence of the nature of polymer–particle surface interactions, the interparticle distance, particle dispersion and particle size on the rheological behaviors. The present work contributes to these issues by constructing a molecular-based model that can be used for quantitative predictions of macroscopic rheological properties of such polymer systems filled with nanoscale particles.

Recent molecular dynamics simulations [1–3] suggested that the polymer–particle surface interactions can be the dominant factor in the rheology of confined systems. These interactions include the short-range forces between the surfaces and the polymer segments, and can be responsible for the suppression of the mobility of polymer segments at the surfaces and even result in the formation of an immobilized glassy layer at the surfaces. Dionne et al. [2] studied the structure and dynamics of an amorphous polyethylene melt containing homogeneously distributed spherical nanoparticles. The polyethylene chains were simulated using both molecular dynamics and Monte Carlo methods. The chain dynamics were monitored by computing the Rouse relaxation modes and the mean-square displacement (MSD). The most notable observation they pointed out, was the slowing down in the Rouse dynamics seen on all subsections of the chain no matter how small the

* Corresponding author.
E-mail addresses: kalonji.kabanemi@cnrc-nrc.gc.ca, kalonji.kabanemi@nrc.ca (K.K. Kabanemi).

0377-0257/$ – see front matter.
doi:10.1016/j.jnnfm.2010.04.006

subsections were, meaning that on average every monomer feels the confinement of the neighboring particles, slowing the relaxation of every chain subsection. They also showed that the slowing down due to polymer–particle energetic interaction was similar for all relaxation modes, independent of their wavelength. Shaffer [4] investigated the effects of chain topology on the dynamics of confined polymer melts by conducting computer simulations. Their results suggested that entanglements are neither induced nor enhanced by confinement between impenetrable adsorbing surfaces. However, Sternstein and Zhu [5] reported experimental studies on the nonlinear viscoelastic properties for composites of fumed silica with various surface treatments. They suggested that the primary mechanism for the high reinforcement levels observed at low strains appear to be the polymer–particle interactions, but not particle agglomeration or percolation and that the polymer–particle interactions result in a change in the entanglement (density and distribution) state of the polymer matrix. Filler particle size also plays a key role. They proposed that temporary bonding of chains to the nanoparticle surface results in trapped entanglements and chain loops (chain with multiple bonding contacts with the nanoparticle). Very recently, Oh and Green [6] presented an experimental study revealing how the relaxation dynamics and glass transition of unentangled polystyrene PS/PS-nanoparticle polymer nanocomposites can be tailored to increase, or decrease in magnitude, through careful control of the molecular parameters of the system, i.e., the nanoparticle volume fraction, nanoparticle size, and grafting chain degree of polymerization. Taken together, these findings show that, polymer–particle surface interactions play an essential role in the dynamics behavior of polymer chains at larger scales. Hence, depending on the polymer–particle energetic interaction and the interparticle distance (the particle volume fraction and size), the mobility of chain segments located on or near nanoparticle surfaces could be considerably slowed down.

Our aim here is to capture this physics in a molecular-based constitutive model on larger scales. A simple way to tackle the dynamics and rheology of polymers filled with nanoparticles is to utilize the ideas of transient networks theories [7]. Along these lines, Inn and Wang [8] applied a transient network model to provide a phenomenological account of some reported rheological behaviors of filled polymer melts. Entanglement points were described by one kind of temporary junctions with lifetime τ_p. Presence of nanoparticles introduced another kind of network junctions with a lifetime τ_s. The degree of compatibility of particle surfaces with the polymer medium was characterized in terms of the adsorption time τ_s relative to the disentanglement time τ_p. The model can explain the variation of shear viscosity with surface treatment of particles and with molecular weight of polymer matrix at a given particle volume fraction. However, the dependence of viscoelastic properties on particle size and interparticle spacing was not captured by the model. Havet and Isayev [9] proposed a rheological model of highly interactive polymer–particle mixtures, based on a double network created by the entangled polymer matrix and the adsorbed polymer. Both networks were represented by a Giesekus constitutive equation. The dependence of rheological properties on particle concentration was taken into account through the bridging density resulting from polymer–particle interactions and a hydrodynamic reinforcement. The relative contribution of both networks was computed through the energy balance consistent with the thermodynamics of the polymer–particle chemical interactions and fluid mechanics. This approach allowed calculating shear rate dependence of stresses under steady simple shear flow and upon start-up and cessation of shear flow. The authors recognized that a further refinement of this model is possible by taking into account kinetics of adsorption–desorption, adsorbed layer thickness, conformation and molecular weight distribution. Sarvestani and Picu [10] proposed a network model for nanofilled polymeric mixtures in the unentangled regime and in which the wall-to-wall distance between nanoparticles is on the order of the chain size. The resulting model captured the main features that distinguish nanocomposite and microcomposite behaviors, for example, the enhanced reinforcement at low deformation rates. More recently, Sarvestani and Picu [11] analysed the dynamics of polymer melts and concentrated solutions reinforced with nanoscale rigid spherical particles. The effects of entanglement were represented by requiring the diffusion in the chain contour direction to be more pronounced than in the direction transverse to the chain primitive path. The influence of polymer–particle interaction was captured within a continuum approximation, in which an attachment point was represented as a region of enhanced friction for the respective chain. Hence, the model is purely frictional in nature. The drawbacks and limitations of the model are related to the homogenized representation of the polymer–particle attachments and the dumbbell simplification used.

Taking advantage of these insights, we use a reptation-based model that incorporates an effective disengagement time to treat the dynamics of chain entanglements in the presence of attractive impenetrable nanoparticles. The model is further refined by adding the nonlinear dynamics of detachment/re-attachment of monomers from/to nanoparticle surfaces under flow conditions. Such a dynamics strongly depends on the polymer–particle affinity, the particle volume fraction, the particle size, and the degree of confinement of polymer chains. The paper is organized as follows: We first propose a mechanism of chain diffusion to estimate the effective curvilinear diffusion coefficient of a polymer chain along its tube in the presence of attractive nanoparticles. Next, we introduce the dynamics of detachment/re-attachment of monomers from/to nanoparticle surfaces under flow conditions. Then, we turn to the prediction of chain conformation by means of the Rouse-CCR tube model [12,13] that incorporates an effective reptation time and an effective Rouse relaxation time. In the subsequent section, we analyse the behavior of the underlying model in step shear strain, steady shear, and start-up of steady shear flow experiments, and perform quantitative comparisons of its behavior to the experimental data of Zhang and Archer [14,15]. A final discussion that includes an extension to a multi-mode version of the model for future improvements concludes the paper.

2. Terminal relaxation time

We start with the reptation motion of an arbitrary polymer chain in an entangled polymer melt. In the standard tube-based model, the main large-scale motion of a polymer chain is its reptation along the tube, which can be viewed as a random sequence of forward and backward displacements along the tube axis, with a certain curvilinear diffusion constant D_c [16,17]

$$D_c = \frac{k_b T}{N\zeta}, \tag{1}$$

where N is the number of monomers or Kuhn segments per polymer chain, ζ is the friction coefficient due to topological interactions, T is the absolute temperature and k_B is the Boltzmann constant.

The contour length of the tube is given by the primitive chain length, consisting of Z primitive path steps (chain segments) which connect two consecutive entanglement points. At equilibrium, the average primitive path step or the tube segment length, l_0, is expected to be of the same order as the equilibrium tube diameter, a, and the equilibrium contour length of the whole tube is written as $L = Zl_0 = Za$. According to Gaussian chain statistics, $al_0 = N_e b^2$ or $a^2 = N_e b^2$, where b is the length of a monomer, N_e is the number of monomers between entanglements at equilibrium and $N = ZN_e$

is the number of monomers per chain. In the reptation theory, the time required for a chain to escape from its tube by curvilinear diffusion, i.e., the disengagement or reptation time, τ_d, is given by

$$\tau_d = \frac{L^2}{D_c} = \left(\frac{Na}{N_e}\right)^2 \frac{1}{D_c} = \frac{\zeta N^3 b^4}{\pi^2 k_B T a^2} = 3\left(\frac{N}{N_e}\right)\tau_R = 3\left(\frac{N}{N_e}\right)^3 \tau_e, \quad (2)$$

where τ_R and τ_e are the Rouse relaxation time of the entire polymer chain with N monomers and the Rouse relaxation time of an entanglement strand, respectively. Based on Eq. (2), the curvilinear diffusion coefficient of the chain along its tube can be expressed as

$$D_c = \frac{1}{3}\left(\frac{a^2}{\tau_e}\right)\frac{N_e}{N}. \quad (3)$$

Let us now consider a system of linear entangled monodisperse polymers and a random uniform distribution of non-aggregated isotropic rigid spherical nanoparticles. A similar model system has been also studied by Zhang and Archer [14] and Sarvestani and Picu [11]. For such a system, molecular simulations [2,10] estimated that a bridging network linking neighboring nanoparticles forms once the wall-to-wall distance between nanoparticles, d_w, approximated by [18]

$$\frac{d_w}{d_f} = \left[\frac{\phi_m}{\phi_f}\right]^{1/3} - 1, \quad (4)$$

was on the order of the average random coil diameter, $2R_g$. In Eq. (4), ϕ_m is the maximum random packing volume fraction, whose value is close to 0.638, d_f is the diameter of nanoparticles and ϕ_f is the nanoparticle volume fraction. Simple calculations show that if the nanoparticles are homogeneously distributed on a cubic lattice in a polymer host and have a diameter of 10 nm at particle volume fraction of about 3%, then the average wall-to-wall distance between nanoparticles, d_w, is about 18 nm. For those filled systems where the particle spacing is comparable to or lower than the average random coil diameter, $2R_g$, any polymer chain may simultaneously attach to more than one nanoparticle in equilibrium configuration, resulting in a bridging network. Such a representation, however, is approximate since real nanoparticles are faceted. This affects the chain structure through the different geometry and through the fact that a faceted particle has a nonuniform propensity for bonding with the polymer chain over its surface [19].

The internal chain scale structure of an attached polymer chain to nanoparticle surfaces may be divided into four components [3]: bridges which start at one nanoparticle surface and end at another nanoparticle surface, attached sections, which have contacts with only one nanoparticle surface, i.e., trains of monomers, which are contiguous series of attached monomers on the nanoparticle surface but their lengths are relatively small; a train is therefore considered as a single contact point [20,21]; loops, which are series of unattached monomers between two trains, and tails, which are chain segments connected at one end to the nanoparticle surface and having the other end free. In the general case these components (bridges, loops and tails) are polydisperse, i.e., they incorporate a different number of monomers. As first approximation, however, we assume that these components incorporate a similar number of monomers. Needless to say, quantitative comparison with experimental data will be affected within the context of single-mode model as presented here.

Obviously, in such a filled system, simple reptation is not possible but, as shown by Zhang and Archer [14], polymer chains may relax via dissociation, i.e., detachment from attractive sites of the nanoparticles, disentanglement from other immobilized chains, or other mechanisms.

In order to estimate the effective reptation time, $\tau_{d,eff}$, of a polymer chain in the presence of attractive nanoparticles, we take a view similar to that presented by Leibler et al. [22] and Vanhoorne and Register [23] to study the dynamics of reversible networks.

An attached monomer is assumed to be characterized by a finite lifetime, τ_g, which reflects the average time which a monomer spends on an attractive site of the nanoparticle surface. For time scales longer than, τ_g, the monomer detaches from an attractive site of the nanoparticle surface (on time scale τ_g) and re-attaches to another attractive site, on time scale, τ_{reatt}, which allows the diffusive motion of the chain segment to which the attached monomer is bound. For a polymer chain which contains a large number of attached monomers, diffusion of the center of mass of the chain will require a very large number of these detachment/re-attachment processes, because these diffusive motions of short chain segments are uncorrelated. This relaxation mechanism allows a polymer chain to make a reptation step without requiring all attached monomers in the polymer chain to be released simultaneously, the probability of which becomes vanishingly small as the number of attached monomers per chain increases.

In line with the above picture, an attached monomer may detach from the nanoparticle surface by a strong thermal fluctuation. If we use the theory of activation process [3], the characteristic time of detachment of a monomer from the nanoparticle surface, i.e., the lifetime of an attached monomer, τ_g, is approximated by

$$\tau_g \cong \tau_0 \exp\left[\frac{U_a - F\alpha}{k_B T}\right], \quad (5)$$

where the front factor, $\tau_0 \sim b(m/k_B T)^{1/2}$, is the characteristic time of molecular oscillation, $1/\tau_g$ represents the rate of detachment process, $U_a \cong \varepsilon k_B T$ is the activation energy of an individual monomer attached to the nanoparticle surface, m is its mass, ε is a parameter representing the monomer–nanoparticle energetic interaction, F is the tensile force in the chain segment, and α is a constant activation length. In writing Eq. (5), it is acknowledged that, in activation processes like that of monomer detachment from attractive nanoparticle surfaces, the lifetime of an adsorbed monomer also depends on tensile force in the strand.

To estimate the effective curvilinear diffusion coefficient, $D_{c,eff}$, of a polymer chain along its tube in the presence of attractive nanoparticles, we argue as follows. At initial time, $t = 0$, the test chain is trapped in a certain tube imposed by the surrounding chains. At the same time, a fraction of the test chain is attached at a certain number of attractive sites of the nanoparticles. According to the reptation theory [16], on the time scales of the order of the reptation time, τ_d, the polymer chain is supposed to disengage from the tube it was confined at $t = 0$. However, in a filled system, because the nanoparticles can be visualized as surrounded by a very high friction region, it is natural to assume that the near-wall segments have a very small mobility, giving rise to a slowing down of the overall reptation motion, through the constraint of chain connectivity.

Inspired by the theory of polymer dynamics for reversible networks [22], let, n_{ad}, be the average number of attached monomers per chain, and, $\phi_{ad} = n_{ad}/N$, the fraction of attached monomers per chain. The average number of monomers along the chain between two successive attached points can be estimated by

$$N_s \cong \frac{N}{n_{ad} + 1}. \quad (6)$$

When one monomer detaches from the nanoparticle surface, i.e., one attached link breaks, a chain segment consisting of $2N_s$ monomers between attached ends of the chain segment undergoes Rouse-like motion. The mean-square curvilinear segment displacement along the tube varies with time as

$$s^2(t) \cong (2N_s)b^2\left[\frac{t}{\tau_R(2N_s)}\right]^{1/2} = N_e b^2\left[\frac{t}{\tau_e}\right]^{1/2} \quad t < \tau_R(2N_s), \quad (7)$$

where the Rouse relaxation time of the chain segment of $2N_s$ monomers is given by

$$\tau_R(2N_s) = \left(\frac{2N_s}{N_e}\right)^2 \tau_e. \tag{8}$$

For times longer than, $\tau_R(2N_s)$, the mean-square curvilinear segment displacement along the tube is constrained by attached ends of the chain segment of $2N_s$ monomers, and the mean-square curvilinear segment displacement is

$$s^2(t) \cong (2N_s)b^2 \quad t > \tau_R(2N_s). \tag{9}$$

On average, after time, τ_{reatt}, the monomer re-attaches such that the maximum curvilinear segment displacement along the tube is, $s(\tau_{reatt})$. Since only a fraction, $1/(n_{ad}+1)$, of the chain is between successive attached points in the chain, the center of mass of the polymer chain moves along the tube by

$$\Delta_c \cong \frac{s(\tau_{reatt})}{n_{ad}+1}. \tag{10}$$

Hence, a sequence of such random elementary steps results in reptation-like diffusion of the polymer chain in the presence of attractive nanoparticles. It is implicitly acknowledged that the dominant process, i.e., the most probable elementary step, is the one involving the detachment of one attached monomer in the chain. Other elementary steps involving simultaneous detachment of many monomers per chain are neglected. For a polymer chain which contains a large number of attached monomers, n_{ad}, diffusion of the center of mass of the chain will require a very large number of these elementary steps, since during these steps, the center of mass of the chain is displaced by a small curvilinear distance. It would be relatively straightforward to modify the model so as to account also for elementary steps involving simultaneous detachment of many monomers per chain. The frequency, ν, of an elementary step involving the detachment of one attached monomer in the chain is given by

$$\nu = \frac{1-\phi_{ad}}{\tau_{reatt}}. \tag{11}$$

During a time span, τ, the average number of these elementary steps per chain will be, $\nu{\cdot}\tau$. Thus, the total mean-square curvilinear displacement of the center of mass of the polymer chain along the tube during time span τ is

$$\Delta^2 = \tau\nu\Delta_c^2. \tag{12}$$

Therefore, the effective curvilinear diffusion coefficient of a chain along its tube in the presence of attractive nanoparticles is

$$D_{c,eff} \cong \frac{\Delta^2}{\tau}. \tag{13}$$

Based on Eqs. (7)–(13), the effective curvilinear diffusion coefficient can be written as

$$D_{c,eff} \cong \frac{N_e b^2}{(\tau_{reatt}\tau_e)^{1/2}} \frac{(1-\phi_{ad})}{(n_{ad}+1)^2} \quad \tau_{reatt} < \tau_R(2N_s), \tag{14}$$

$$D_{c,eff} \cong \frac{(2N_s)b^2}{\tau_{reatt}} \frac{(1-\phi_{ad})}{(n_{ad}+1)^2} \quad \tau_{reatt} > \tau_R(2N_s). \tag{15}$$

In the limit of a completely free chain, $n_{ad} \to 0$, while the strand of $2N_s$ monomers corresponds to the full chain of N monomers and, τ_{reatt}, plays the role of the Rouse relaxation time of the full chain, $\tau_R(N)$. Hence, the effective curvilinear diffusion coefficient, as given by Eqs. (14) and (15), reduces to the standard curvilinear diffusion coefficient, i.e.,

$$D_{c,eff} \cong \left(\frac{a^2}{\tau_e}\right)\frac{N_e}{N}. \tag{16}$$

The effective reptation time, $\tau_{d,eff}$, of a polymer chain in the presence of attractive nanoparticles corresponds to the displacement along the tube on a distance of order of the total tube length, i.e., $L = aN/N_e$. Therefore

$$\tau_{d,eff} = \left(\frac{aN}{N_e}\right)^2 \frac{1}{D_{c,eff}}. \tag{17}$$

Combining Eqs. (14) to (17) we get

$$\tau_{d,eff} \cong \left(\frac{N}{N_e}\right)^2 (\tau_{reatt}\tau_e)^{1/2} \frac{(n_{ad}+1)^2}{(1-\phi_{ad})} \quad \tau_{reatt} < \tau_R(2N_s), \tag{18}$$

$$\tau_{d,eff} \cong \left(\frac{N^2}{N_e}\right) \frac{1}{(2N_s)} \tau_{reatt} \frac{(n_{ad}+1)^2}{(1-\phi_{ad})} \quad \tau_{reatt} > \tau_R(2N_s). \tag{19}$$

The effective reptation time, $\tau_{d,eff}$, is related to the reptation time, τ_d, of a chain in the neat polymer as

$$\tau_{d,eff} \cong \tau_d \frac{2N_s}{N} \left[\frac{\tau_{reatt}}{\tau_R(2N_s)}\right]^{1/2} \frac{(n_{ad}+1)^2}{(1-\phi_{ad})} \quad \tau_{reatt} < \tau_R(2N_s), \tag{20}$$

$$\tau_{d,eff} \cong \tau_d \frac{2N_s}{N} \frac{\tau_{reatt}}{\tau_R(2N_s)} \frac{(n_{ad}+1)^2}{(1-\phi_{ad})} \quad \tau_{reatt} > \tau_R(2N_s). \tag{21}$$

By neglecting numerical prefactors in Eqs. (20) and (21), the effective reptation time, $\tau_{d,eff}$, is seen to scale with molecular weight as $\tau_{d,eff} \sim \tau_d(\phi_{ad}N+1)^2$, which indicates that the overall relaxation is extremely retarded by attractive nanoparticles in the limit of strongly adsorbed chain, i.e., $n_{ad} >> 1$.

In the limit of a completely free chain, $n_{ad} \to 0$, the effective reptation time, as given by Eqs. (20) and (21), reduces to the reptation time, τ_d, of a chain in the neat polymer system, i.e.,

$$\tau_{d,eff} \cong \left(\frac{N}{N_e}\right)^3 \tau_e. \tag{22}$$

We also use the effective curvilinear diffusion coefficient of the chain along its tube, $D_{c,eff}$, to estimate the effective Rouse relaxation of the chain as

$$\tau_{R,eff} \cong \frac{\tau_{d,eff}}{3Z}. \tag{23}$$

In writing Eq. (23), it is implicitly acknowledged that the presence of nanoparticles leads to changes in all relaxation processes in the same way, independent of their wavelength. This issue was investigated by Dionne et al. [2] who studied the structure and dynamics of an amorphous polyethylene melt containing homogeneously distributed spherical nanoparticles, using both molecular dynamics and Monte Carlo methods.

Finally, the number of attached monomers per chain, n_{ad}, can be estimated from molecular parameters as

$$n_{ad} = \phi_{ad}N \cong \frac{n_{seg}}{n_{chain}}, \tag{24}$$

where n_{seg} and n_{chain} are the number of attached monomers per unit volume and the number of chains per unit volume, respectively. These quantities are defined by

$$n_{seg} = \theta_a n_a, \tag{25}$$

and

$$n_{chain} = (1-\phi_f)\frac{\rho N_A}{M_w}, \tag{26}$$

where θ_a is the nanoparticle coverage, i.e., the fraction of attractive sites on the nanoparticle surface occupied by monomers, n_a is the number of the attractive sites per unit volume, i.e., the number density of attractive sites, ϕ_f is the nanoparticle volume fraction, M_w is the molecular weight of the polymer chain, ρ is the weight of the polymer per unit volume, and $N_A = 6.023 \times 10^{23}\ \mathrm{mol}^{-1}$ is the Avogadro number.

Let n_{as} be the number of attractive sites per unit surface of the nanoparticle, and n_{af} the number of attractive sites per nanoparticle. Then we have

$$n_{af} = n_{as} S_f = \pi\, n_{as} d_f^2, \tag{27}$$

where S_f and d_f are the surface and the diameter of nanoparticles, respectively. Let $n_f = \phi_f / v_f$ be the number of nanoparticles per unit volume, where v_f is the volume of a nanoparticle. Then the number density of attractive sites, n_a, can be defined as follows

$$n_a = n_f n_{af} = \frac{6\,\phi_f n_{as}}{d_f}. \tag{28}$$

The above equation shows that the number density of attractive sites, n_a, increases with decreasing the nanoparticle dimension, d_f, at constant nanoparticle volume fraction, ϕ_f. Combining Eqs. (24) to (28), we get

$$n_{ad} = \phi_{ad} N \cong 6\frac{\phi_f}{1-\phi_f}\frac{\theta_a n_{as}}{\rho N_A d_f} M_w = 6\frac{\phi_f}{1-\phi_f}\frac{\theta_a n_{as}}{\rho N_A d_f}\frac{C_\infty m_0}{(0.82)^2} N, \tag{29}$$

which predicts N scaling for the number of attached monomers per chain, n_{ad}. Hence, the effective reptation, $\tau_{d,eff}$, given by Eqs. (20) and (21) can be written explicitly as

$$\tau_{d,eff} \cong \tau_d \frac{2N_s}{N}\left[\frac{\tau_{reatt}}{\tau_R(2N_s)}\right]^{1/2} \frac{[6(\phi_f/(1-\phi_f))(\theta_a n_{as}/\rho N_A d_f)(C_\infty m_0/(0.82)^2)N+1]^2}{(1-\phi_{ad})} \quad \tau_{reatt} < \tau_R(2N_s) \tag{30}$$

$$\tau_{d,eff} \cong \tau_d \frac{2N_s}{N}\frac{\tau_{reatt}}{\tau_R(2N_s)} \frac{[6(\phi_f/(1-\phi_f))(\theta_a n_{as}/\rho N_A d_f)(C_\infty m_0/(0.82)^2)N+1]^2}{(1-\phi_{ad})} \quad \tau_{reatt} > \tau_R(2N_s) \tag{31}$$

It is apparent from Eqs. (30) and (31) that the effective reptation time, $\tau_{d,eff}$, can be controlled through five main parameters, i.e., the molecular weight of the polymer chain, N, the size of the nanoparticles, d_f, the density of attractive site on the nanoparticle surface, n_{as}, the monomer–nanoparticle energetic interaction, ε, and the particle volume fraction, ϕ_f.

3. Detachment/re-attachment dynamics

In the preceding section, we examined the overall relaxation of a polymer chain adsorbed to attractive nanoparticle surfaces, in the equilibrium configuration. Under flow conditions, the detachment process is favored by the tension in the chain, and this enables the polymer chain to move more easily. This is accompanied with a corresponding decrease of the activation energy. Hence, depending on the flow strength, the instantaneous average number of attached monomers per chain, $n_{ad}(t)$, may be different from the average number of attached monomers per chain, $n_{ad,eq}$, in the equilibrium configuration. It should be emphasized that the equilibrium value, $n_{ad,eq}$, also represents the maximum number of monomers that can be attached per chain.

We now move on to the dynamics of the detachment/re-attachment processes of monomers from/to the nanoparticle surface, which also involves several contributions. Let us first introduce the instantaneous average fraction of attached monomers per chain, $\phi_{ad}(t) = n_{ad}(t)/N$. This number serves as an approximate measure of the degree of attachment of a chain to attractive sites of the nanoparticle surfaces. Here, we make a simplification in describing adsorbed configurations by a single parameter, ϕ_{ad}. A more complete description would also include the location of the attached monomers along the chain backbone as well the position of the unattached monomers of the chain with respect to the surface of the nanoparticles.

Let us now consider a polymer chain with a fraction ϕ_{ad} of attached monomers and let us determine the rate at which this fraction changes with time. In our simplified approach, the kinetic equation of the fraction of attached monomers per chain, ϕ_{ad}, in an average sense, can be obtained by first noting that the detachment process depends on the tensile force in the strand, as imposed by the macroscopic flow, i.e., due to hydrodynamic drag on it from the mean-field friction of surroundings chains, while the re-attachment process is independent of the force in the strand.

An attached monomer can be detached from an attractive site of the nanoparticle by a strong thermal fluctuation. The lifetime of an attached monomer also depends on the tensile force in the strand as given by Eq. (5). Hence the detachment process is characterized by the following equation

$$\frac{d\phi_{ad}}{dt} = -\frac{1}{\tau_g}\phi_{ad} + \frac{1}{\tau_{g,eq}}\phi_{ad,eq}, \tag{32}$$

where, $\phi_{ad,eq} = n_{ad,eq}/N$, is the average fraction of attached monomers per chain in the equilibrium configuration, τ_g is the lifetime of a loaded monomer as defined by Eq. (5), and $\tau_{g,eq}$, is the lifetime time of an unloaded monomer, i.e., in equilibrium configuration. Eq. (32) ensures relaxation to, $\phi_{ad,eq}$.

The detachment process due to thermal fluctuations and macroscopic flow, also occurs concurrently with the re-attachment process of monomers residing in the bulk polymer by some activation process, and is characterized by the following equation

$$\frac{d\phi_{ad}}{dt} = \frac{1}{\tau_{reatt}}(\phi_{ad,eq} - \phi_{ad}), \tag{33}$$

where τ_{reatt}, represents the mean time during which a monomer stays at its own initial position in the bulk polymer before migrating to the final state (trapped configuration), i.e., $1/\tau_{reatt}$, is the rate at which a monomer lives its initial state in the bulk polymer and re-attaches to the nanoparticle surface. The re-attachment time is independent of the force in the strand. Eq. (33) also ensures relaxation to, $\phi_{ad,eq}$.

Hence, the instantaneous average fraction of attached monomers per chain, ϕ_{ad}, is governed by competitive detachment/re-attachment processes by the following kinetic equation:

$$\frac{d\phi_{ad}}{dt} = -\frac{1}{\tau_g}\phi_{ad} + \frac{1}{\tau_{reatt}}\left[\left(\frac{\tau_{reatt}}{\tau_{g,eq}} + 1\right)\phi_{ad,eq} - \phi_{ad}\right]. \tag{34}$$

It is apparent from Eqs. (30), (31) and (34) that the effective reptation time under flow conditions, $\tau_{d,eff}$, depends on the dynamics of detachment/re-attachment of monomers through ϕ_{ad}, which is itself a measure of the instantaneous average number of attached monomers per chain. This approach allows us to discuss, in a transparent manner, the role of different molecular parameters involved, i.e., the energetic interaction parameter between the polymer chain and the nanoparticle surface, the particle volume fraction, the geometrical characteristics of nanoparticles, the fraction of adsorbed monomers, and the molecular weight of the polymer chain.

Finally, as far as the re-attachment process is concerned, let U_b be the activation energy for an individual monomer residing in the bulk polymer. In order to re-attach a monomer residing in the bulk polymer to an attractive site, the polymer chain has to overcome a potential barrier, U_b, much smaller than the activation energy, $U_a \cong \varepsilon k_B T$, of an individual monomer attached to the nanoparticle surface. Hence, the characteristic time of re-attachment, τ_{reatt}, for a monomer residing in the bulk polymer is written as

$$\tau_{reatt} \cong \tau_0 \exp(U_b/k_B T). \tag{35}$$

4. Constitutive equation

We now turn to the prediction of polymer chain conformation. In this analysis we do not consider particle agglomeration or percolation and assume that the filling fraction is small enough for particle–particle interactions to be insignificant. Stress due to particle–particle interactions is also neglected.

It was found in the previous section that the effective reptation time under flow conditions scales with N as $\tau_{d,eff} \sim \tau_d[\phi_{ad}(t)N+1]^2$. In addition, molecular dynamics simulations [2] demonstrated that the presence of nanoparticles leads to changes in all relaxation processes in the same way, independent of their wavelength. Hence, one may use a tube-based model, with an effective reptation time, as given by Eqs. (30) and (31), to mimic the conformational changes of chains in filled systems. Here, we use the Rouse-CCR tube model for linear entangled polymers (Rolie–Poly), as developed by Likhtman and Graham [12] and modified by Kabanemi and Hétu [13]. We include in a simple way the effect of polymer–particle energetic interactions through an effective reptation time $\tau_{d,eff}$, and an effective Rouse relaxation time, $\tau_{R,eff}$, that incorporate the dynamics of detachment/re-attachment through Eq. (34). Hence, for a polymer system filled with nanoscale rigid particles, the conformation of the polymer chain, $\boldsymbol{\sigma}$, in a flow field, $\boldsymbol{u}$, evolves in time by an equation of the form

$$\dot{\boldsymbol{\sigma}} = \boldsymbol{L}\cdot\boldsymbol{\sigma} + \boldsymbol{\sigma}\cdot\boldsymbol{L}^T + \boldsymbol{f}(\boldsymbol{\sigma}), \tag{36}$$

where

$$\boldsymbol{f}(\boldsymbol{\sigma}) = -\frac{1}{\tau_{d,eff}}(\boldsymbol{\sigma}-\boldsymbol{I}) - \frac{2}{\tau_{R,eff}}k_s(\lambda)\left(1-\sqrt{\frac{3}{tr\boldsymbol{\sigma}}}\right)\left(\boldsymbol{\sigma}+\beta\left(\frac{tr\boldsymbol{\sigma}}{3}\right)^{\delta}(\boldsymbol{\sigma}-\boldsymbol{I})\right), \tag{37}$$

and the corresponding stress is taken to be of the form

$$\boldsymbol{\tau} = Gk_s(\lambda)(\boldsymbol{\sigma}-\boldsymbol{I}). \tag{38}$$

Here $\boldsymbol{L} = \nabla\boldsymbol{u}^T$ is the transpose of velocity gradient tensor, β is the CCR coefficient analogous to the coefficient introduced by Marrucci in his original CCR paper [24], δ a negative power which can be obtained by fitting to the full theory, $\boldsymbol{\tau}$ is the polymeric stress contribution, G is the plateau modulus, $k_s(\lambda)$ is the nonlinear spring coefficient accounting for the finite extensibility of polymer chains, equals unity for linear springs and becomes much greater than unity as the spring becomes nearly fully stretched, $\lambda = \sqrt{tr\boldsymbol{\sigma}/3}$ is the chain stretch ratio, $\lambda = 1$ is its equilibrium value in the absence of flow, and $\boldsymbol{\sigma} = \boldsymbol{I}$ is the equilibrium value of the conformation tensor in the absence of flow.

The nonlinear spring coefficient, $k_s(\lambda)$, is approximated by the normalized Padé inverse Langevin function [25], i.e.,

$$k_s(\lambda) = \frac{(3-\lambda^2/\lambda_{\max}^2)(1-1/\lambda_{\max}^2)}{(1-\lambda^2/\lambda_{\max}^2)(3-1/\lambda_{\max}^2)}, \tag{39}$$

where $\lambda_{\max}$ is the maximum stretch ratio.

Let $\boldsymbol{R}$ be the end-to-end vector of the subchain. The entropic force in each subchain is given by

$$\boldsymbol{F}(\boldsymbol{R}) = \frac{3k_BT}{N_eb^2}k_s(\lambda)\boldsymbol{R} = \frac{3k_BT}{a^2}k_s(\lambda)\boldsymbol{R}, \tag{40}$$

whose magnitude can be written as

$$F(R) = \frac{3k_BT}{N_e^{1/2}b}k_s(\lambda)\lambda = \frac{3k_BT}{a}k_s(\lambda)\lambda. \tag{41}$$

Notice that, the dynamics of the detachment/re-attachment processes enters in the constitutive equation, Eq. (36), through the effective reptation time, $\tau_{d,eff}$, and the effective Rouse relaxation time, $\tau_{R,eff}$, while the rate of breaking of monomer-particle bonds, $1/\tau_g$, in Eqs. (5) and (34) is coupled to the chain configuration through Eq. (41).

5. Numerical results

5.1. Step shear strain

To get insight into the dynamics of nanocomposite systems, we analyse the stress relaxation following a step shear strain, $\gamma = \gamma_0 H(t)$, where $H(t)$ is the Heaviside unit step function. For small shear strain, γ_0, the relaxation modulus is found to be independent of γ_0 and the shear stress, τ_{xy}, is linear in strain. The response of this flow defines the relaxation modulus, $G(t) = \tau_{xy}(t)/\gamma_0$. This relaxation modulus can be Fourier transformed in the linear regime, to yield frequency-dependent elastic modulus, $G'(\omega) = \omega\int_0^\infty \sin(\omega t)G(t)dt$ and loss modulus, $G''(\omega) = \omega\int_0^\infty \cos(\omega t)G(t)dt$, over a wide frequency range.

A standard polyethylene oxide (PEO) with a molecular weight $M_w = 189,000$ g/mol and various PEO/silica nanocomposites are first analysed. These polymer systems are similar to those investigated in the experiments by Zhang and Archer [14]. The model parameters are summarized in Table 1. Some of the parameters, i.e., N, b, and G were calculated from molecular parameters of the neat PEO as given by Fetters et al. [26], while the nanoparticle characteristics are those given by Zhang and Archer [14] and Kawaguchi et al. [27]. The activation length, α, is assumed to be on the order of a Kuhn segment. The reptation time, τ_d, of the neat PEO was estimated from the data given by Zhang and Archer, while $\beta = 1$ and $\delta = -0.5$ are the optimal values to fit both transient and steady state predictions of the neat polymer system [12]. Although the model includes the Rouse time, the linear viscoelastic response of the model does not extend up to frequencies where the dominating dynamics is Rouse-like. In what follows, we examine the effects of the nanoparticle volume fraction, ϕ_f, the monomer-particle energetic interaction parameter, ε, and the initial fraction of attached monomers, $\phi_{ad}(t=0)$. For the sake of brevity, we only focus on the elastic properties of various mixtures and will not discuss the results for the loss modulus, $G''(\omega)$.

The linear viscoelastic properties are presented in Fig. 1 for $\varepsilon = 25$, $\phi_{ad}(t=0) = 0$, $\tau_{reatt}/\tau_{g,eq} = 10^{-2}$, and various particle volume fractions ϕ_f. At frequencies higher than $10\,s^{-1}$, the storage moduli, $G'(\omega)$, of the neat polymer and the nanocomposite systems are essentially the same and exhibit a solid-like behavior. At low frequency, the terminal behaviors of the neat polymer and nanocomposite systems are very different. The neat polymer exhibits a liquid-like behavior with the typical slope, equal to 2. In the long time region (low frequency), it is observed that the relaxation is slowed down by the presence of nanoparticles. The rate of slowing down increases monotonically with increase of the particle volume fraction. The storage moduli of the nanocomposite systems at various nanoparticle volume fractions are several times higher than that of the neat polymer. With increasing the

Table 1
Typical PEO/silica nanocomposite polymer system used in this study.

Parameters	Values PEO (M_w = 189,000 g/mol)
N	1570
b (nm)	0.581
d_f (nm)	12
n_{as} (1/nm^2)	2
θ_a	0.2
τ_d (s)	0.2
τ_R (s)	1.59×10^{-3}
G (Pa)	18×10^5

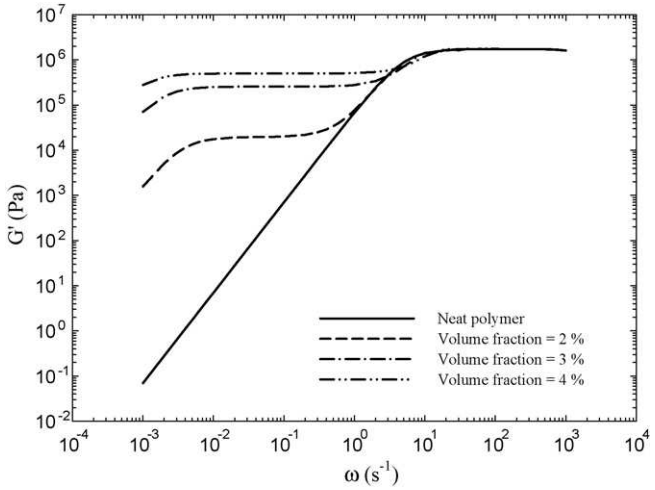

Fig. 1. Frequency dependence of storage modulus, $G'(\omega)$, for the neat polymer system and the nanocomposite systems. Effect of the particle volume fraction, ϕ_f, at fixed monomer–particle energetic interaction parameter, $\varepsilon = 25$.

particle volume fraction, the storage modulus, $G'(\omega)$, exhibits a second low-frequency plateau (solid-like behavior), whose height is lower than the high-frequency plateau. The width of the second plateau region increases with increasing the particle volume fraction, while the transition point depends essentially on the dynamics of detachment/re-attachment of monomers from/to the nanoparticle surfaces and to the initial value of the fraction of adsorbed monomers per chain, $\phi_{ad}(t=0)$. Since the effective reptation time scales with, N, as $\tau_{d,eff} \sim \tau_d[\phi_{ad}(t)N+1]^2$, the liquid-like behaviors are exhibited only at very low-frequency region (long time region), for nanocomposite systems studied here. This behavior has been demonstrated in the experiments of Zhang and Archer [14], and will be further discussed in the section on experimental validation of the model.

The effect of the monomer-particle energetic interaction parameter, ε, at fixed particle volume fraction, equal to 2% and $\phi_{ad}(t=0) = \phi_{ad,eq}$, is analysed in Fig. 2. As the energetic parameter, ε, increases, the width of the plateau region (solid-like behavior) increases. This behavior clearly demonstrates that, the rheological properties of nanocomposite systems depend critically on the adsorption of monomers to the surface of nanoparticles. This observation is supported by previous findings [2,14], which show that

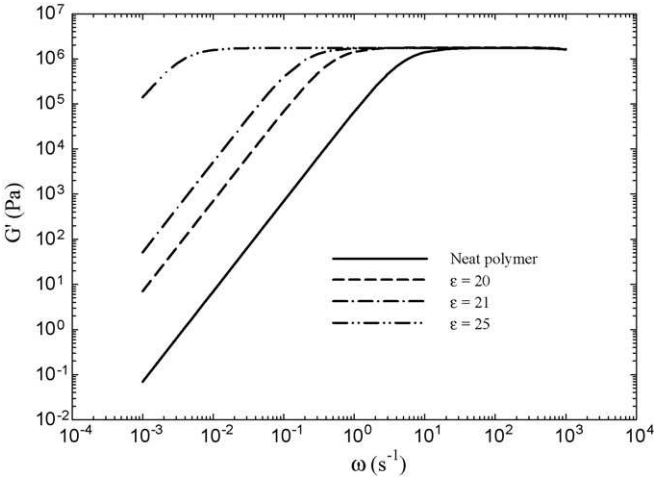

Fig. 2. Frequency dependence of storage modulus, $G'(\omega)$, for the neat polymer system and the nanocomposite systems. Effect of the monomer–particle energetic interaction parameter, ε, at fixed particle volume fraction, equal to 2%.

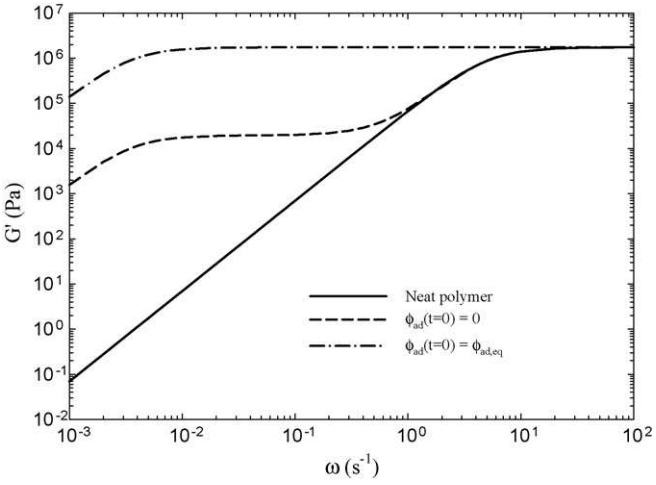

Fig. 3. Frequency dependence of storage modulus, $G'(\omega)$, for the neat polymer system and the nanocomposite systems. Effect of the initial fraction of attached monomers $\phi_{ad}(t=0)$, at fixed particle volume fraction, equal to 2% and fixed monomer–particle energetic interaction parameter, $\varepsilon = 25$.

nanocomposites properties depend strongly on surface properties of nanoparticles.

The effect of the initial fraction of attached monomers, $\phi_{ad}(t=0)$, at fixed particle volume fraction, equal to 2% and fixed monomer-particle energetic interaction parameter, $\varepsilon = 25$, is analysed in Fig. 3. It is seen that the low-frequency plateau region increases with increasing the initial fraction of attached monomers. When the initial fraction of attached monomers per chain is close to zero, the overall relaxation time depends strongly on the dynamics of detachment/re-attachment, while a constant rate of relaxation is exhibited for the initial fraction of attached monomers per chain close to the equilibrium value, i.e., $\phi_{ad}(t=0) = \phi_{ad,eq}$.

5.2. Steady shear flow

We examine in this section the material functions for a steady shear flow described by a velocity field, $u = \dot{\gamma} y$, where $\dot{\gamma}$ is the steady shear rate. As in the preceding investigation, the model parameters are summarized in Table 1. In Fig. 4, we show the shear rate dependence of the viscosity for the neat polymer and the nanocomposite systems at $\varepsilon = 20$, $\tau_{reatt}/\tau_{g,eq} = 0.1$ and vari-

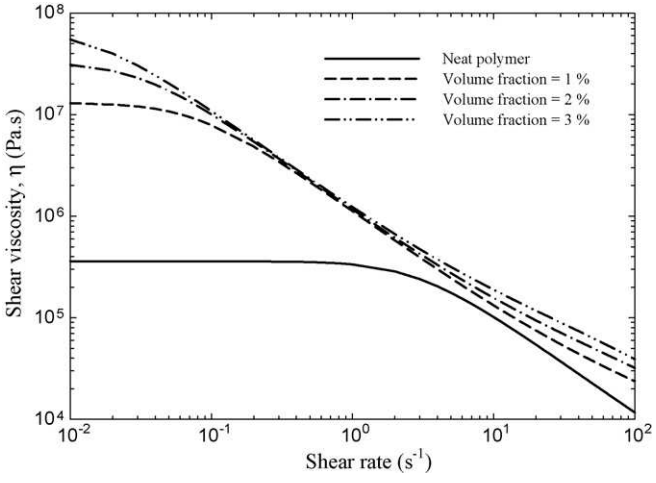

Fig. 4. Shear rate dependence of the steady shear viscosity, η, for the neat polymer system and the nanocomposite systems. Effect of the particle volume fraction, ϕ_f, at fixed monomer–particle energetic interaction parameter, $\varepsilon = 20$, and fixed ratio, $\tau_{reatt}/\tau_{g,eq} = 0.1$.

ous particle volume fractions ϕ_f. While the neat polymer exhibits a Newtonian behavior up to $\dot{\gamma} = 1$, the nanocomposite systems exhibit the shear thinning behavior at low shear rates. Even at very low particle volume fractions, ϕ_f, the zero-shear viscosities of the nanocomposite systems are dramatically increased, due to a larger flow stress experienced by polymer chains. This behavior can be explained by the flow restrictions arising from the presence of nanoparticles that decreases the effective curvilinear diffusion coefficient, and leads to a reduction of the average mobility of polymer chains. At high shear rates, as the detachment of monomers is intensified by the macroscopic flow, the neat polymer dominates the shear thinning behavior, suggesting that the presence of nanoparticles contributes negligible to the viscosity in strong flows. A more careful scrutiny of Fig. 4 reveals that, at very high shear rates regime, the slope of the shear thinning of nanocomposite systems is dominated both by the detachment of monomers from the nanoparticle surfaces and the degree of chain stretching, as the effective reptation time and the effective Rouse relaxation time strongly depend on the degree of attachment of chains to attractive sites, ϕ_{ad}, and on the nanoparticle loadings. Therefore, the relaxation dynamics of the filled system is slowed down, leading to early orientation and stretching of sub-chains compared to the neat system. Furthermore, at low shear rates, because polymer chains are trapped by more than one nanoparticle, orientation of sub-chains in the flow direction is enhanced with increasing nanoparticle volume fraction, ϕ_f. This is reflected by the early shear thinning exhibited by these mixtures. In addition, the shear rate at which the non-Newtonian behavior is initiated decreases with increasing the particle volume fractions, ϕ_f. At high shear rates, the detachment process makes the steady shear viscosity decrease, approaching that of the neat polymer with a slope which depends on the particle volume fraction. The steady shear viscosities of the neat polymer and those of the nanocomposite systems tend to merge, demonstrating that at these high shear rates the neat polymer dominates the shear thinning behavior. These results are supported by recent experimental data of Zhang and Archer [15], who investigated the rheological behavior of semidilute aqueous dispersions of polyethylene oxide containing nanosized silica particles.

In Fig. 5 we show the steady shear stress as a function of shear rate, for the neat polymer and the nanocomposite systems at different levels of nanoparticle loading. The model predicts a monotone increase of the steady shear stress with increasing particle volume fraction, also seen in the experiments of Havet and Isayev [28]. In

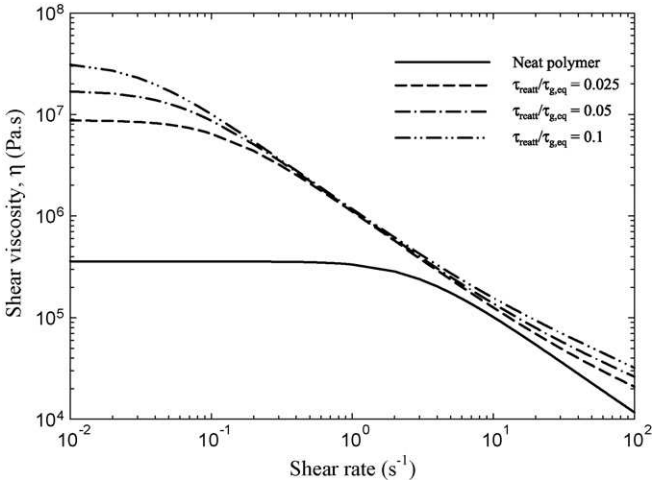

Fig. 6. Shear rate dependence of the steady shear viscosity, η, for the neat polymer system and the nanocomposite systems. Effect of the ratio, $\tau_{reatt}/\tau_{g,eq}$, at fixed monomer–particle energetic interaction parameter, $\varepsilon = 20$, and fixed particle volume fraction, equal to 2%.

the low shear rate range, the plateau region for the two nanocomposite systems with the highest nanoparticle loading is mainly dominated by the orientation of sub-chains, indicative of the existence of the yield stress for these filled systems. As mentioned above, at low shear rates, the overall relaxation time of the polymer chain increases with increasing nanoparticle volume fraction, as a polymer chain may attach simultaneously to more nanoparticles. This, in turn, is reflected in the enhancement of orientation of chain segments in the flow direction, at low shear rates, as also highlighted in Fig. 4. As mentioned above, both the effective reptation time and the effective Rouse relaxation time increase with the nanoparticle loadings and the monomer-particle interactions, leading to early orientation and stretching of sub-chains.

In Fig. 6, we analyse the effect of the ratio, $\tau_{reatt}/\tau_{g,eq}$, on the steady shear viscosity at fixed nanoparticle volume fraction equal to 2%, and fixed energetic interaction parameter equal to 20. The zero-shear viscosities exhibit a monotonic increase with increasing the ratio, $\tau_{reatt}/\tau_{g,eq}$. By increasing the shear rate, the viscosities of all filled systems exhibit the shear thinning behaviors.

In Fig. 7 we examine the dynamics of detachment/reattachment of monomers from/to nanoparticle surfaces. The steady

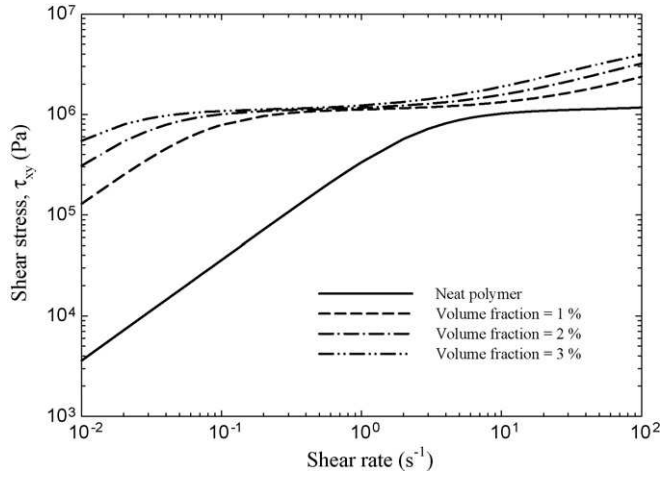

Fig. 5. Shear rate dependence of the steady shear stress, τ_{xy}, for the neat polymer system and the nanocomposite systems. Effect of the particle volume fraction, ϕ_f, at fixed monomer–particle energetic interaction parameter, $\varepsilon = 20$, and fixed ratio, $\tau_{reatt}/\tau_{g,eq} = 0.1$.

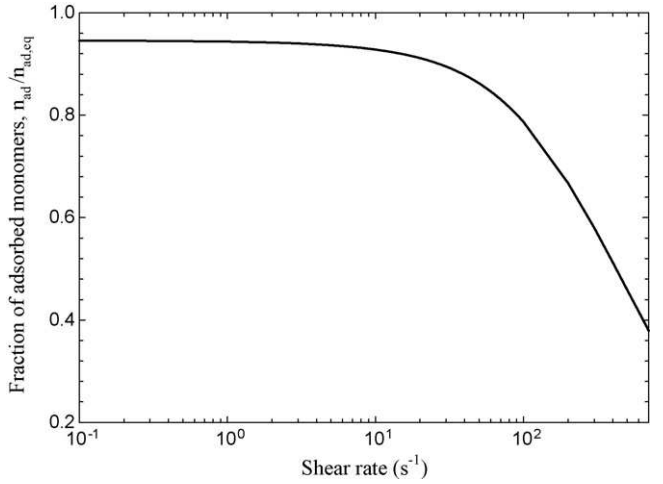

Fig. 7. Shear rate dependence of the fraction of adsorbed monomers per chain, $\eta_{ad}/\eta_{ad,eq}$ for the model nanocomposite system, at fixed ratio, $\tau_{reatt}/\tau_{g,eq} = 0.1$, fixed monomer-particle energetic interaction parameter, $\varepsilon = 20$, and fixed particle volume fraction, equal to 2%.

state fraction of attached monomers per chain, $n_{ad}/n_{ad,eq}$, exhibits a plateau at low strain rates, with the value of $n_{ad}/n_{ad,eq}$, close to unity, reflecting that the detachment process is only marginal in this flow range. For fast flows, the detachment process is intensified by the tensile force in the strand. Therefore, trapped monomers are relaxed, and $n_{ad}/n_{ad,eq}$, exhibits an exponential reduction, suggesting that, in rapidly changing flows, on average, the behavior is mainly dominated by that of the neat system.

The dependence of the steady shear viscosity on the energetic interaction parameter, ε, at fixed particle volume fraction, equal to 2% and fixed ratio, $\tau_{reatt}/\tau_{g,eq} = 0.1$, is shown in Fig. 8. The results are markedly similar to the behavior seen in nanocomposite systems at various particle volume fractions. The enhancement of the zero-shear rate viscosity is solely due to the increase of the energetic parameter, i.e., monomer-nanoparticle surface interactions, since particle–particle interactions are not included in the model. At low ε, adsorption of monomers to the nanoparticle surfaces is insignificant and thus the effective curvilinear diffusion coefficient is only marginally affected. In such a situation, the shear viscosity is insensitive to the presence of nanoparticles, and the steady shear viscosity of the neat polymer is recovered. As we increase the value of the energetic interaction parameter, ε, the nanocomposite systems exhibit a strong shear thinning behavior at very low shear rates, as a result of a decrease of the effective curvilinear diffusion coefficient, i.e., an increase of the effective reptation time. These surface interactions act to reduce the overall mobility of polymer chains. The degree of slowing increases with the strength of the interaction, as reflected by the early shear thinning exhibited by these mixtures in Fig. 8. This strongly suggests that the energetic polymer–particle interaction is a key parameter for the observed non-Newtonian behavior and the large enhancement seen in the zero-shear viscosities, at relatively low particle volume fractions. Hence, even at very low shear rates, significant orientation of tube segments in the flow direction occurs, that is reflected in the premature shear thinning behavior exhibited. Therefore particle orientation, as such, has nothing to do with the observed non-Newtonian behavior, as only isotropic spherical nanoparticles are considered.

The present analysis, based on a typical polymer filled with nanoscale rigid particles, provides a plausible explanation for some rheological behavior reported previously [15,28], namely, slower relaxation of polymer chains with the addition of the nanoparticles, low-frequency plateau (solid-like behavior), enhancement of shear viscosity at low shear rates, and the independence of the steady shear stress on the shear rate at low shear rates, i.e., the existence of a yield stress. The current model also reproduces the dynamics of detachment/re-attachment of monomers from/to nanoparticle surfaces, and provides a physical explanation of the observed rheological behaviors in strong flows. It is clear that there is no unique route to the huge alteration seen in rheological properties, and that the detailed behavior of real nanocomposites depends also on the shape of the nanoparticles, the level of dispersion, the surface treatment, etc.

Finally, it is fair to recall that the present model is based on a restrictive approximation for the internal chain scale structure, i.e., bridges, loops and tails are assumed to be monodisperse. In the general case these components are polydisperse. It would be necessary to extend our model so as to remove this simplification by using a multi-mode model.

5.3. Start-up of steady shear flow

The flow is described by a velocity field, $u = \dot{\gamma}(t)y$, where $\dot{\gamma}(t)$ is a time dependent shear rate represented by a step function $\dot{\gamma}(t) = \dot{\gamma}_0 H(t)$. The model parameters are summarized in Table 1. In Fig. 9 we show the evolution of the shear viscosity, $\eta^+(t)$, for $\dot{\gamma}_0 = 0.1\,s^{-1}$, $\phi_{ad}(t=0) = \phi_{ad,eq}$, at a fixed energetic polymer–particle interaction parameter, $\varepsilon = 20$, a fixed ratio, $\tau_{reatt}/\tau_{g,eq} = 0.1$, and various particle volume fractions. As we increase the nanoparticle volume fraction, ϕ_f, the transient shear viscosities exhibit overshoots whose magnitudes increase with nanoparticle loading and then decrease to the steady state. The analogous diagram of the transient first normal stress differences, $N_1^+(t)$, is shown in Fig. 10. These results predict no overshoot and large steady state values of the first normal stress differences as ϕ_f increases. The dependence of shear viscosity, $\eta^+(t)$, on the energetic interaction parameter ε, for $\dot{\gamma}_0 = 0.1\,s^{-1}$, $\phi_{ad}(t=0) = \phi_{ad,eq}$, at a fixed particle volume fraction, equal to 3%, and a fixed ratio, $\tau_{reatt}/\tau_{g,eq} = 0.1$, is shown in Fig. 11. As ε is increased, an overshoot is exhibited, similar to the effect of nanoparticle loading.

5.4. Experimental validation

We here perform a quantitative comparison with the experimental data reported by Zhang and Archer [14,15], for the neat PEO and various PEO/silica nanocomposites. The model parame-

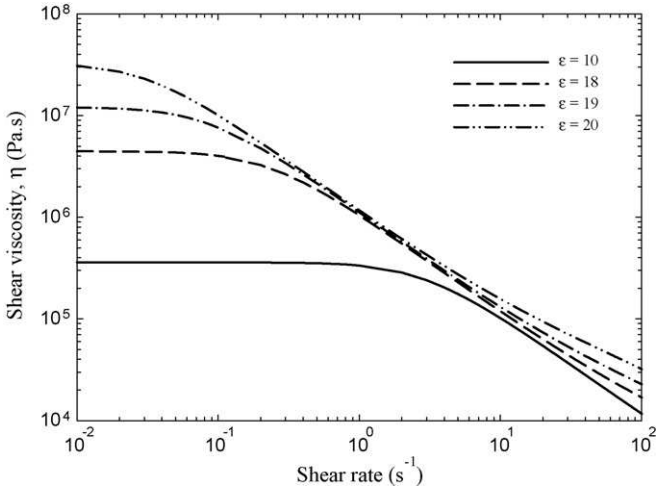

Fig. 8. Shear rate dependence of the steady shear viscosity, η, for the nanocomposite systems. Effect of the monomer–particle energetic interaction parameter, ε, at fixed particle volume fraction, equal to 2%, and fixed ratio, $\tau_{reatt}/\tau_{g,eq} = 0.1$.

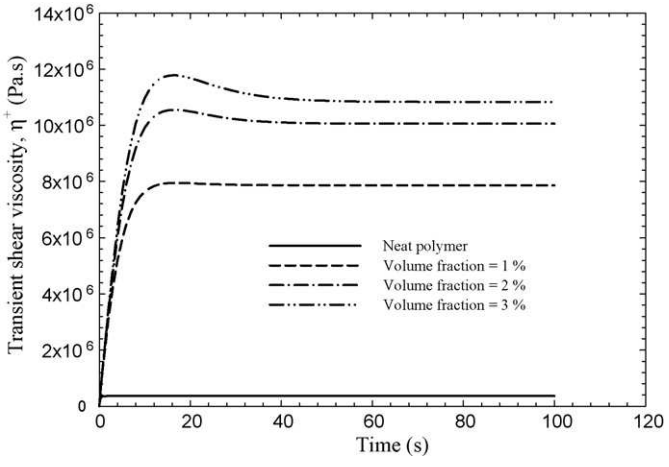

Fig. 9. Transient shear viscosity, $\eta^+(t)$, during start-up of steady shear for the neat polymer system and the nanocomposite systems, for $\dot{\gamma}_0 = 0.1\,s^{-1}$. Effect of the particle volume fraction ϕ_f, at fixed monomer–particle energetic interaction parameter, $\varepsilon = 20$, fixed ratio, $\tau_{reatt}/\tau_{g,eq} = 0.1$, and $\phi_{ad}(t=0) = \phi_{ad,eq}$.

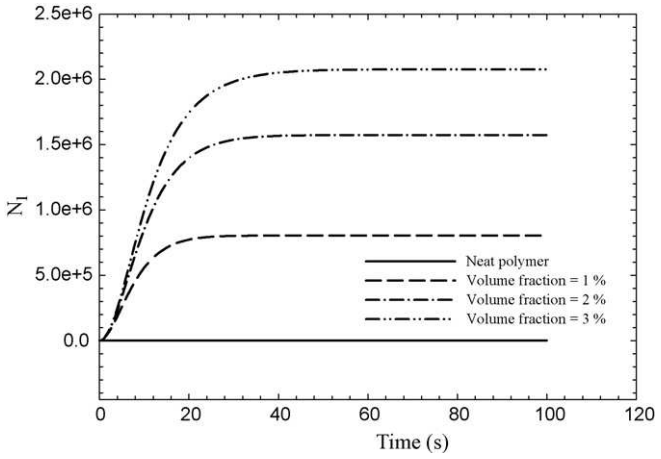

Fig. 10. Transient first normal stress difference, $N_1^+(t)$, during start-up of steady shear for the neat polymer system and the nanocomposite systems, for $\dot{\gamma}_0 = 0.1\,s^{-1}$. Effect of the particle volume fraction ϕ_f, at fixed monomer–particle energetic interaction parameter, $\varepsilon = 20$, fixed ratio, $\tau_{reatt}/\tau_{g,eq} = 0.1$, and $\phi_{ad}(t=0) = \phi_{ad,eq}$.

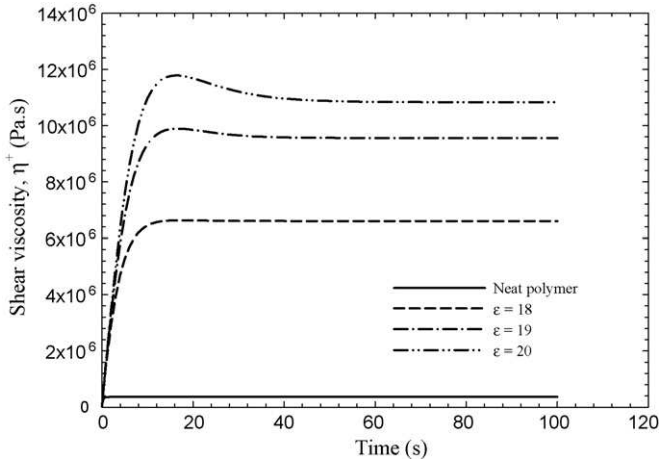

Fig. 11. Transient shear viscosity, $\eta^+(t)$, during start-up of steady shear for the neat polymer system and the nanocomposite systems, for $\dot{\gamma}_0 = 0.1\,s^{-1}$. Effect of the monomer–particle energetic interaction parameter, ε, at fixed particle volume fraction, equal to 3%, fixed ratio, $\tau_{reatt}/\tau_{g,eq} = 0.1$, and $\phi_{ad}(t=0) = \phi_{ad,eq}$.

ters are summarized in Table 2. Some of the parameters, i.e., N and b, were calculated from molecular parameters of the neat PEO as given by Fetters et al. [26], while the nanoparticle characteristics are those given by Zhang and Archer [14] and Kawaguchi et al. [27]. The energy parameter, ε, can be determined by fitting the dynamic rheological behaviors of the neat PEO and PEO/silica nanocomposites at various temperatures. Simple calculations show that if the nanoparticles of diameter of about 12 nm are homogeneously distributed on a cubic lattice in a polymer host with a random coil diameter, $2R_g = 20$ nm (PEO/silica nanocomposite P189-S4), at particle volume fraction of about 4%, then the average wall-to-wall distance between nanoparticles, d_w, is about 18 nm. This implies that for the filled systems analysed here and by Zhang and Archer, any polymer chain may simultaneously attach to more than one nanoparticle in equilibrium configuration, resulting in a bridging network.

Table 2
PEO/silica nanocomposites data: P189 and P700 (Zhang and Archer [14,15]).

Parameters	Values	
	PEO P189 (M_w = 189,000 g/mol)	PEO P700 (M_w = 700,000 g/mol)
N	1570	5821
b (nm)	0.581	0.581
d_f (nm)	12	12
θ_a	0.2	0.15
ε	25	21
τ_d (s)	0.2	3×10^{-4}

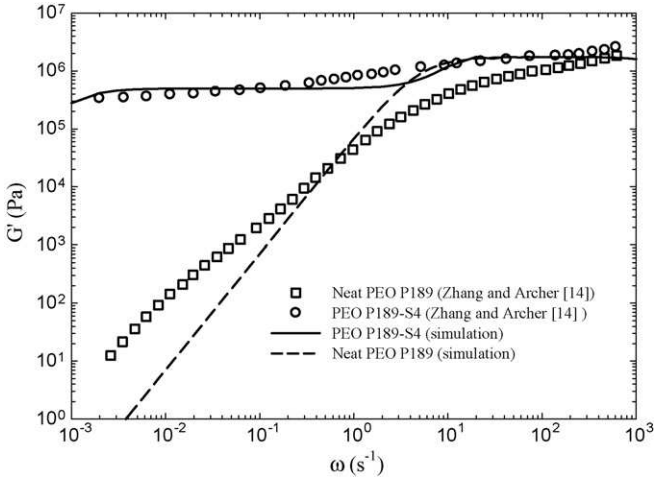

Fig. 12. Frequency dependence of storage modulus, $G'(\omega)$, for the neat PEO P189 and the PEO/silica nanocomposites P189-S4 ($\phi_f = 4\%$). Comparison of numerical predictions and experimental data of Zhang and Archer [14].

In Fig. 12, we show a comparison of the model predictions and the experimental data for the storage modulus as a function of frequency, for the neat PEO P189 and the PEO/silica nanocomposite P189-S4 ($\phi_f = 4\%$) [14]. We first note that the low-frequency storage modulus is highly sensitive to the particle volume fraction. Even at very low nanoparticle volume fraction, the storage modulus of the nanocomposite system is several times higher than that of the neat polymer, and exhibits a clear second low-frequency plateau (solid-like behavior), whose height is lower than the high-frequency plateau. This behavior is a result of the coupled effects of monomer–nanoparticle energetic interactions, nanoparticle volume fraction, and nanoparticle diameter. The deviation from the limiting slope (≈2) at low frequency, for the neat polymer, is due to polydispersity, while the high-frequency range is independent of this, and the high-frequency plateau modulus is unaffected. These results show that the present model is able to correctly reproduce the linear viscoelastic behaviors of such complex mixtures.

The dependence of the steady shear viscosity on shear rate, for the neat PEO P700 and various PEO/silica nanocomposites [15], is shown in Fig. 13. Quantitative predictions of the model are impressive. At low shear rates, all PEO systems exhibit a clear Newtonian behavior, while PEO/silica nanocomposites with various particle volume fractions exhibit non-Newtonian shear thinning behavior with increasing shear rates. This behavior is mainly governed by the dynamics of detachment/re-attachment of monomers from/to nanoparticle surfaces, and suggests that, in PEO/silica nanocomposites, tube segments start to orient towards the flow direction even at low shear rates, as a result of the increase of the effective reptation time, due to monomer-particle interactions. We also observe that even at relatively low particle loading, $\phi_f = 1\%$, the zero-shear rate viscosity is already enhanced by a factor of about 3. Zhang and Archer [15] showed that the dispersion with $\phi_f = 2\%$, gives a 750% zero-shear rate viscosity increase compared to that of the pure PEO solution. The Einstein equation, $\eta(\phi_f) = 1 + 2.5\phi_f$, gives only a 5% viscosity increase, suggesting that PEO/silica nanocomposites behave far from colliding hard spheres in a continuum medium. In addition, at 2% volume fraction and an average nanoparticle diameter, $d_f = 12$ nm, the wall-to-wall distance between the nanoparticles

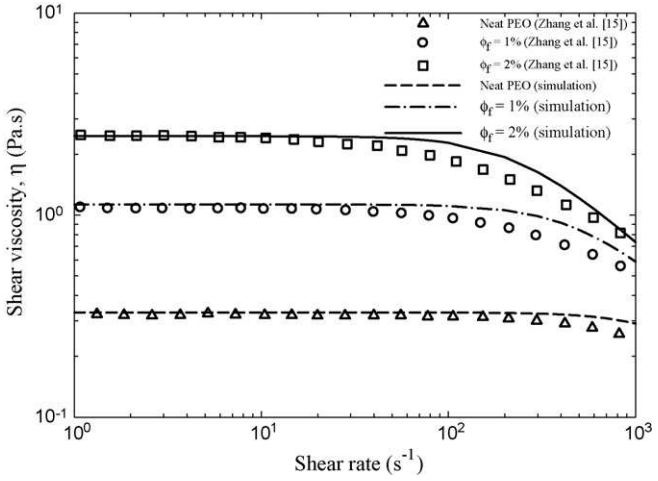

Fig. 13. Shear rate dependence of the steady shear viscosity, η, for the neat PEO P700 and the PEO/silica nanocomposites. Comparison of numerical predictions and experimental data of Zhang and Archer [15].

is, $d_w = 26$ nm, while the equilibrium polymer coil diameter is $2R_g = 60$ nm, implying that significant level of confinement exists in these nanocomposite systems. Furthermore, for particle loadings investigated here, any polymer chain may simultaneously attach to more than one nanoparticle in equilibrium configuration, resulting in a bridging network. One would also anticipate that at very high shear rates, the viscosities of the neat PEO solution and those of the PEO/silica nanocomposites will merge, as the detachment process will dominate over the re-attachment one. The present numerical prediction results suggest that the polymer–particle interactions, their dynamics under flow conditions, i.e., the detachment/re-attachment processes, and the degree of confinement of polymer chains are the key factors for the observed enhancements both of the zero-shear rate viscosity and the elastic modulus, and also the strong non-Newtonian shear thinning behaviors exhibited.

6. Discussion

As we have seen the single-mode model developed in this study has predicted many aspects of the linear and nonlinear viscoelastic data of well characterized PEO/silica nanocomposite systems where any polymer chain simultaneously attaches to one or more nanoparticles in equilibrium configuration, resulting in a bridging network. For example, simple calculations show that if the nanoparticles of diameter of about 12 nm are homogeneously distributed on a cubic lattice in a polymer host with a random coil diameter, $2R_g = 20$ nm (PEO/silica nanocomposite P189-S4), at particle volume fraction of about 4%, then the average wall-to-wall distance between nanoparticles, d_w, is about 18 nm, that is, smaller than $2R_g$. For such model systems, the single-mode model developed here for a monodisperse distribution of chains in the presence of rigid nanoparticles, has found success in predicting the experimental data. However, as emphasized in Section 2, such a representation is approximate since real nanocomposite systems are largely polydisperse, that is, they contain chains with a wide range of relaxation times, some are attached to nanoparticles and others are free, affecting the overall dynamics and rheological behavior. In addition, as mentioned in Section 2, the internal chain scale structure of an attached chain to nanoparticle surfaces contains bridges, loops and tails. In the general case these components are polydisperse, i.e., they incorporate a different number of monomers.

Summarizing, the model presented in this study strictly applies only to model systems of linear monodisperse chains and a uniform distribution of non-aggregated rigid spherical nanoparticles, in which: (i) the average wall-to-wall distance between nanoparticles is on the order of the chain size; (ii) in equilibrium any chain simultaneously attaches to one or more nanoparticles, i.e., all chains are assumed to behave in the same way; they all have the same reptation time, and the same Rouse relaxation time.

It would be necessary to extend our model so as to remove these simplifications by using a multi-mode model that incorporates attached and free chains. In what follows we shall limit ourselves to the basic of the extended model, leaving the numerical results and quantitative comparison to a forthcoming paper.

6.1. Diffusion of an attached chain

Having described the basic mechanism of reptation-like diffusion of a polymer chain in the presence of attractive nanoparticles in Section 2, we shall now make a generalization of that theory. A schematic representation of the internal structure of an attached chain is shown in Fig. 14. For simplicity, we shall assume that an attached point may represent a junction between two successive bridges with the probability P_{BB}, or a junction between a bridge and a loop with the probability P_{BL}, or a junction between a bridge and a tail with the probability P_{BT}, or a junction between two successive loops with the probability P_{LL}, or a junction between a loop and a tail with the probability P_{LT}, or a junction between two successive tails with the probability P_{TT}. These are the probabilities associated with the various scenarios for an attached point of an adsorbed chain. Needless to say, the sum of these probabilities is one. We proceed by assuming that, under equilibrium configuration, these quantities are known or can be determined by molecular dynamics simulations [10,29].

Now let n_B and n_L be the average number of bridges and loops per chain, respectively. In equilibrium configuration, these quantities can be estimated by

$$n_B \cong n_{ad}\left(P_{BB} + \frac{P_{BL}}{2} + \frac{P_{BT}}{2}\right), \tag{42}$$

and

$$n_L \cong n_{ad}\left(P_{LL} + \frac{P_{BL}}{2} + \frac{P_{LT}}{2}\right). \tag{43}$$

Following the mechanism of reptation outlined in Section 2, when one attached link breaks, a chain segment consisting of $2N_s$ monomers between attached ends of the chain segment undergoes Rouse-like motion. The mean-square curvilinear segment displacement along the tube varies with time as

$$s^2(t) \cong (2N_s)b^2\left[\frac{t}{\tau_R(2N_s)}\right]^{1/2} = N_e b^2\left[\frac{t}{\tau_e}\right]^{1/2} \quad t < \tau_R(2N_s), \tag{44}$$

$$s^2(t) \cong (2N_s)b^2 \quad t > \tau_R(2N_s), \tag{45}$$

where the average number of monomers, $2N_s$, along the chain segments is now estimated by

$$2N_s(n_{ad}) \cong 2N_B P_{BB} + (N_B + N_L)P_{BL} + (N_B + N_T)P_{BT} + 2N_L P_{LL} + (N_L + N_T)P_{LT} + 2N_T P_{TT}. \tag{46}$$

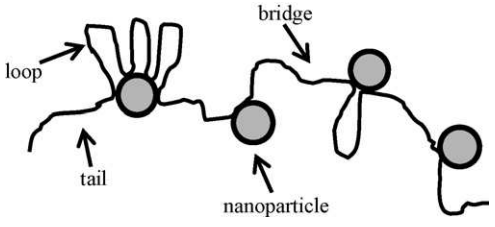

Fig. 14. Schematic representation of the internal structure of an attached chain.

In Eq. (46), N_B, N_L and N_T represent the average number of monomers per bridge, loop and tail, respectively. This result can then be used to determined the effective curvilinear diffusion coefficient, $D_{c,eff}$, following the same procedure outlined in Section 2.

If we assume that under equilibrium configuration all components, i.e., bridges, loops and tails, incorporate a similar number of monomers, N_s, with the same probability, then the monodisperse result, $2N_s(n_{ad}) = 2N_s$, is recovered from Eq. (46).

On the other hand, under nonequilibrium conditions, it is not unreasonable to assume that the probability, P_{BB}, to find an attached link in the chain which connects two successive bridges, follows the same dynamics as that of ϕ_{ad}, Eq. (34). Thus, we have

$$P_{BB}(t) = P_{BB,eq}\frac{n_{ad}(t)-1}{n_{ad,eq}-1} \quad n_{ad}(t) \geq 1, \tag{47}$$

The other probabilities also follow the same dynamics, i.e., the probability P_{BL} to find an attached link in the chain which connects a bridge and a loop, or the probability P_{BT} to find an attached link in the chain which connects a bridge and a tail, or the probability P_{LL} to find an attached link in the chain which connects two successive loops, or the probability P_{LT} to find an attached link in the chain which connects a loop and a tail. Conversely, the probability, P_{TT}, to find an attached link in the chain which connects two successive tails is given by the constraint

$$P_{TT} = 1 - (P_{BB} + P_{BL} + P_{BT} + P_{LL} + P_{LT}). \tag{48}$$

While the average number of monomers per bridge, N_B, and the average number of monomers per loop, N_L, are assumed to remain constant during deformation, a decrease in the average number of bridges, n_B, and loops, n_L, per chain due to the detachment process of an attached chain from nanoparticles, only induces an increase in the average number of monomers per tail, N_T. Under these conditions, the average number of monomers per tail, N_T, can be approximated by

$$N_T \cong \frac{N-(n_B N_B + n_L N_L)}{2}. \tag{49}$$

In writing Eq. (49), it is implicitly assumed that, an attached chain always contains two tails.

According to this model, in strong flows, as the instantaneous average number of attached monomers per chain, $n_{ad}(t)$, approaches 1, the probability to find a bridge or a loop in the chain is nearly zero, while the probability to find a tail, $P_{TT} \to 1$. In this regime, the dynamics is associated with those of tails and free chains, only.

The present theory is essentially a phenomenological one and involves various assumptions. Our major assumption is that, the detachment process of an adsorbed chain induced by the flow proceeds from bridges or loops closer to chain-ends to those internal. As a consequence, a reduction in the number of bridges and loops per chain results in an increase in the number of monomers per tail, N_T, while the equilibrium values N_B and N_L remain unchanged. We know that the real picture is more complicated because, a more complete description would also include the location of the attached monomers along the chain backbone, i.e., the location of bridges and loops, as well the position of the unattached monomers of the chain with respect to the surface of the nanoparticles. Of course, there are various possibilities of other generalizations that can be pursued.

6.2. Multi-mode constitutive equation

To mimic the effects of polydispersity of a filled system that incorporates attached chains to nanoparticles and free ones, a multi-mode version of the model presented in Section 4 is used. The polydisperse Rolie–Poly model that we present here is a trivial extension of the monodisperse model obtained by taking the stress to be a weight-average of the stresses obtained for each chain type of the composite, i.e., attached and free chains. For a polymer system filled with nanoscale rigid particles, the conformation of the polymer chain, $\boldsymbol{\sigma}_i$, in a flow field, $\boldsymbol{u}$, evolves in time by an equation of the form

$$\dot{\boldsymbol{\sigma}}_i = \boldsymbol{L}\cdot\boldsymbol{\sigma}_i + \boldsymbol{\sigma}_i\cdot\boldsymbol{L}^T + \boldsymbol{f}_i(\boldsymbol{\sigma}_i), \tag{50}$$

where

$$\boldsymbol{f}_i(\boldsymbol{\sigma}_i) = -\frac{1}{\tau_{d,i}}(\boldsymbol{\sigma}_i - \boldsymbol{I}) - \frac{2}{\tau_{R,i}}k_{s,i}(\lambda_i)\left(1-\sqrt{\frac{3}{tr\boldsymbol{\sigma}_i}}\right)\left(\boldsymbol{\sigma}_i + \beta\left(\frac{tr\boldsymbol{\sigma}_i}{3}\right)^{\delta}(\boldsymbol{\sigma}_i - \boldsymbol{I})\right), \tag{51}$$

and the total stress is taken to be of the form

$$\boldsymbol{\tau} = \sum_{i=a,f} w_i G_i k_{s,i}(\lambda_i)(\boldsymbol{\sigma}_i - \boldsymbol{I}). \tag{52}$$

Here the subscripts $i = a$ and $i = f$ denote components of attached and free chains, respectively, w_i is the weight fraction of chains of type i, $\tau_{d,i=a} = \tau_{d,eff}$, and $\tau_{R,i=a} = \tau_{R,eff}$, are the reptation and the Rouse relaxation times, respectively, of attached chains, while $\tau_{d,i=f} = \tau_d$, and $\tau_{R,i=f} = \tau_R$, are the reptation and the Rouse relaxation times, respectively, of free chains.

In the limit of very strong flows where, $n_{ad} \to 0$, $\tau_{d,eff} = \tau_d$, and $\tau_{R,eff} = \tau_R$, implying that attached chains behave like free ones, and the underlying model, Eqs. (50)–(52), reduce to the standard single-mode model proposed previously as a special case, Eqs. (36)–(38).

7. Conclusions

Our aim in this study was in mesoscopic rheological modeling of nanocomposite systems. We developed a reptation-based model that incorporates polymer–particle interactions and confinement, to describe the dynamics and rheological behaviors of linear entangled polymers filled with isotropic nanoscale particles. The model predicted a scaling law in the form, $\tau_{d,eff} \sim \tau_d(\phi_{ad}N+1)^2$, where $\tau_{d,eff}$ is the effective reptation time of a chain in the presence of attractive nanoparticles, τ_d is its reptation time in the neat polymer, ϕ_{ad} is the fraction of attached monomers per chain, and N is the number of monomers per chain. Hence, the overall relaxation is extremely retarded by attractive nanoparticles in the limit of strongly adsorbed chains. Also, it was found that the effective reptation time, $\tau_{d,eff}$, can be controlled through five main parameters, i.e., the molecular weight of the polymer chain, N, the size of the nanoparticles, d_f, the density of attractive site on the nanoparticle surface, n_{as}, the monomer-nanoparticle energetic interaction, ε, and the nanoparticle volume fraction, ϕ_f.

An important additional physics that was incorporated in this study was the nonequilibrium dynamics of detachment/reattachment of monomers from/to nanoparticle surfaces under flow conditions. This approach allowed us to discuss, in a transparent way, the role of different parameters involved, i.e., the energetic interaction parameter between the polymer chain and the nanoparticle surface, the particle volume fraction, the interparticle distance, the geometrical characteristics (shape) of the nanoparticles, the fraction of adsorbed monomers, and the molecular weight of the polymer chain. The resulting model correctly captured the linear dynamical properties and shear rheological behaviors of nanocomposite systems studied. The high viscosity exhibited at low shear rates can be explained by the flow restrictions arising from the presence of nanoparticles that decreases the effective curvilinear diffusion coefficient. Under slow shear flow conditions, these

filled systems exhibit a strong non-Newtonian behavior and a large enhancement in the viscosity as a certain number of monomers in the chain are attached to nanoparticle surfaces. At high shear rates, the neat polymer dominates the shear thinning behavior, suggesting that addition of nanoparticles contributes negligible to the viscosity in strong flows. These results also suggest that the energetic polymer–particle interaction, the particle size and the degree of confinement are the key parameters for the observed non-Newtonian behavior and the large enhancement in the viscosity of such filled systems. For these systems, significant orientation of tube segments in the flow direction is predicted at low shear rates. This behavior is reflected in the early shear thinning exhibited. Therefore, according to the present model, particle orientation, as such, has nothing to do with the observed non-Newtonian behavior, since only isotropic spherical nanoparticles were considered. The nonlinear viscoelasticity is also greatly affected by the dynamics of detachment/re-attachment of monomers from/to nanoparticle surfaces, as the effective reptation time and the effective Rouse relaxation time strongly depend on the degree of attachment of chains to attractive sites and on the nanoparticle loadings.

Acknowledgments

The results presented in this work have been obtained within the framework of the NRC-NSERC-BDC Nanotechnology Initiative. The authors would like to thank the anonymous reviewers of the manuscript for their constructive comments that contributed to the quality of this work.

References

[1] C.R. Picu, A. Rakshit, Dynamics of free chains in polymer nanocomposites, J. Chem. Phys. 126 (2007) 144909–144911.
[2] P.J. Dionne, R. Ozisik, C.R. Picu, Structure and dynamics of polyethylene nanocomposites, Macromolecules 38 (2005) 9351–9358.
[3] A. Subbotin, A. Semenov, M. Doi, Friction in strongly confined polymer melts: effect of polymer bridges, Phys. Rev. E 56 (1997) 623–630.
[4] J.S. Shaffer, Dynamics of confined polymer melts: topology and entanglement, Macromolecules 29 (1996) 1010–1013.
[5] S.S. Sternstein, A.J. Zhu, Reinforcement mechanism of nanofilled polymer melts as elucidated by nonlinear viscoelastic behavior, Macromolecules 35 (2002) 7262–7273.
[6] H. Oh, P.F. Green, Polymer chain dynamics and glass transition in athermal polymer/nanoparticle mixtures, Nat. Mater. 8 (2009) 139–143.
[7] G.G. Fuller, L.G. Leal, Network model of concentrated polymer solutions derived from the Yamamoto network theory, J. Polym. Sci. Polym. Phys. Ed. 19 (1981) 531–555.
[8] Y.-W. Inn, S.Q. Wang, Transient network model for a multiphase polymeric fluid, Rheol. Acta 32 (1993) 581–588.
[9] G. Havet, A.I. Isayev, A thermodynamic approach to the rheology of highly interactive filler-polymer mixtures. Part I. Theory, Rheol. Acta 40 (2001) 570–581.
[10] A.S. Sarvestani, C.R. Picu, Network model for the viscoelastic behavior of polymer nanocomposites, Polymer 45 (2004) 7779–7790.
[11] A.S. Sarvestani, C.R. Picu, A frictional molecular model for the viscoelasticity of entangled polymer nanocomposites, Rheol. Acta 45 (2005) 132–141.
[12] A.E. Likhtman, R.S. Graham, Simple constitutive equation for linear polymer melts derived from molecular theory: Rolie–Poly equation, J. Non-Newtonian Fluid Mech. 114 (2003) 1–12.
[13] K.K. Kabanemi, J.F. Hétu, Nonequilibrium stretching dynamics of dilute and entangled linear polymers in extensional flow, J. Non-Newtonian Fluid Mech. 160 (2009) 113–121.
[14] Q. Zhang, L.A. Archer, Poly(ethylene oxide)/silica nanocomposites: structure and rheology, Langmuir 18 (2002) 10435–10442.
[15] Q. Zhang, L.A. Archer, Optical polarimetry and mechanical rheometry of poly(ethylene oxide)-silica dispersions, Macromolecules 37 (2004) 1928–1936.
[16] M. Doi, S.F. Edwards, The Theory of Polymer Dynamics, Oxford University Press, Oxford, 1986.
[17] A.N. Semenov, M. Rubinstein, Dynamics of strongly entangled polymer systems: activated reptation, Eur. Phys. J. B 1 (1998) 87–94.
[18] A. Tuteja, M.E. Mackay, C.J. Hawker, B. Van Horn, Effect of ideal, organic nanoparticles on the flow properties of linear polymers: non-Einstein-like behavior, Macromolecules 38 (2005) 8000–8011.
[19] C.R. Picu, M.S. Ozmusul, Structure of linear polymeric chains confined between impenetrable spherical walls, J. Chem. Phys. 118 (2003) 11239–11248.
[20] K.A. Smith, M. Vladkov, J.L. Barrat, Polymer melt near a solid surface: a molecular dynamics study of chain conformations and desorption dynamics, Macromolecules 38 (2005) 571–580.
[21] A.L. Yarin, M.D. Graham, A model for slip at polymer/solid interfaces, J. Rheol. 42 (1998) 1491–1504.
[22] L. Leibler, M. Rubinstein, R.H. Colby, Dynamics of reversible networks, Macromolecules 24 (1991) 4701–4707.
[23] P. Vanhoorne, R.A. Register, Low-shear melt rheology of partially-neutralized ethylene-methacrylic acid ionomers, Macromolecules 29 (1996) 598–604.
[24] G. Marrucci, Dynamics of entanglements: a nonlinear model consistent with the Cox-Merz rule, J. Non-Newtonian Fluid Mech. 62 (1996) 279–289.
[25] C. Pattamaprom, J.J. Driscroll, R.G. Larson, Nonlinear viscoelastic predictions of uniaxial-extensional viscosities of entangled polymers, Macromol. Symp. 158 (2000) 1–13.
[26] L.J. Fetters, D.J. Lohse, D. Richter, T.A. Witten, A. Zirkel, Connection between polymer molecular weight, density, chain dimensions, and melt viscoelastic properties, Macromolecules 27 (1994) 4639–4647.
[27] M. Kawaguchi, K. Maeda, T. Kato, A. Takahashi, Preferential adsorption of monodisperse polystyrene on silica surface, Macromolecules 17 (1984) 1671–1678.
[28] G. Havet, A.I. Isayev, A thermodynamic approach to the rheology of highly interactive filler-polymer mixtures. Part II. Comparison with polystyrene/nanosilica mixtures, Rheol. Acta 42 (2003) 47–55.
[29] M.S. Ozmusul, C.R. Picu, S.S. Sternstein, S.K. Kumar, Lattice Monte Carlo simulations of chain conformations in polymer nanocomposites, Macromolecules 38 (2005) 4495–4500.